ELSEVIER

Journal of Structural Geology 26 (2004) 2251–2267

JOURNAL OF STRUCTURAL GEOLOGY

www.elsevier.com/locate/jsg

A linkage criterion for segmented normal faults

Roger Soliva*, Antonio Benedicto

Lab. Orsayterre, Université Paris XI, FRE 2566, Bât. 504, 91405 Orsay cedex, France

Received 28 May 2003; received in revised form 26 February 2004; accepted 10 June 2004

Abstract

A detailed field study of 39 centimetre- to metre-scale relay ramps from two outcrops was performed to investigate the development of a linkage criterion for segmented normal faults. We analysed the displacement distribution and the geometry of fault arrays containing three types of relay ramp: open, linked, and fully breached, in order to identify which parameters are relevant to fault linkage, and to establish a linkage criterion. Each relay ramp geometry has a specific graphical field on a *relay displacement–separation* diagram. The field including all the linked geometries (initiation of linkage) separates open and fully breached relay ramps and is interpreted as a value of *relay displacement* to *separation* ratio for which faults link during their overlap. A 'linkage threshold', in each studied fault system, is defined as the best-fit linear trend of linked relays. We discuss the scaling and the variability of the linkage criterion using published datasets from a wide variety of settings and scales. The observed linkage threshold is linear, with a slope value varying less than one order of magnitude. This suggests that linking relay ramps have self-similar geometries from centimetre- to kilometre-scale and that normal fault linkage is governed by similar fault interaction across a broad range of scales. The linkage criterion, which can be an effective tool to estimate relay ramp geometry at depth or at the earth surface, could therefore be used to improve investigations in determining fluid entrapment or in the evaluation of potential surface of seismic ruptures.

Keywords: Normal fault; Segment; Relay ramp; Linkage; Prediction

1. Introduction

Across a broad range of scales, normal faults are observed as isolated (Fig. 1a) and frequently as discontinuous sub-parallel stepping segments (Fig. 1b) separated by relay ramps (Fig. 1c), also called relay zones (Huggins et al., 1995), overlap zones (Childs et al., 1995) or transfer zones (Morley et al., 1990). The relay ramp is a rotated volume between two normal fault segments that overstep along strike and that have the same dip direction (Larsen, 1988; Peacock and Parfitt, 2002). In the past decade, many papers have focused on understanding the evolution of these relay ramps. These works were motivated by several reasons:

(1) To improve comprehension of mechanical interaction and linkage processes between normal faults (Peacock and Sanderson, 1991; Bürgmann et al., 1994; Trudgill and Cartwright, 1994; Huggins et al., 1995; Willemse et al., 1996; Willemse, 1997; Crider and Pollard, 1998; Gupta and Scholz, 2000; Ferrill and Morris, 2001; Peacock, 2002). This approach includes: implications for surface topography and architecture of sedimentary deposits (Gawthorpe and Hurst, 1993; Gupta et al., 1999; Morley, 1999; Young et al., 2001); effect on scaling laws and growth models of normal faults (Peacock and Sanderson, 1991; Childs et al., 1995; Dawers and Anders, 1995; Cartwright et al., 1996; Wojtal, 1996; Marchal, 1997; Mansfield and Cartwright, 2001); and effects on fault size and spatial distribution (Cladouhos and Marret, 1996; Nicol et al., 1996; Cowie, 1998; Schultz, 2000; Ackermann et al., 2001).
(2) To better determine fluid entrapment and migration in faulted reservoirs (Morley et al., 1990; Gawthorpe and Hurst, 1993; Peacock and Sanderson, 1994; Maerten et al., 2000), because relay ramps can be leakage zones or barriers to fluid flow from the hanging wall to the footwall. Furthermore, relay ramps can be important

* Corresponding author. Tel.: +33-169156797; fax: +33-169154911
E-mail address: soliva@geol.u-psud.fr (R. Soliva).

0191-8141/$ - see front matter © 2004 Elsevier Ltd. All rights reserved.
doi:10.1016/j.jsg.2004.06.008

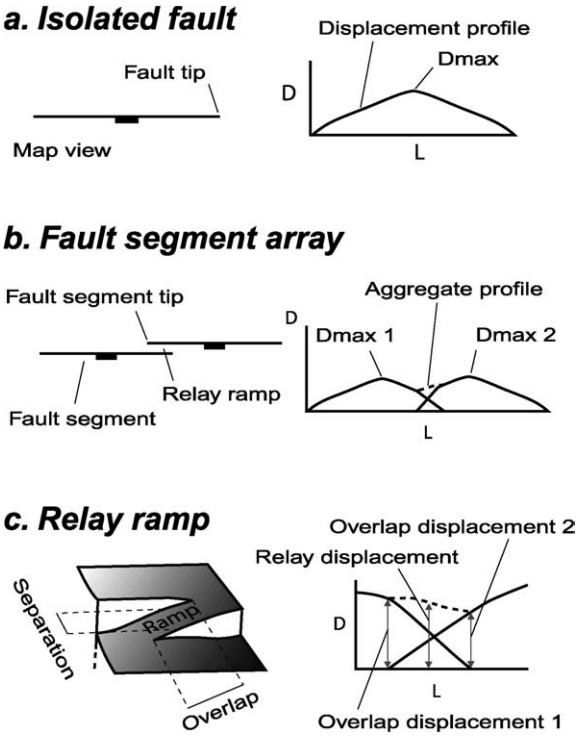

Fig. 1. Terminology used in the paper. (a) Map view and associated displacement profile (distribution of the displacement, *D*, along the fault length, *L*) of an isolated fault ('non-interacting' fault in the terms of Gupta and Scholz (2000)). D_{max} is the maximum value of displacement. (b) Map view and associated displacement profile of a fault array containing two segments. 'Fault segment array' is defined as the entire geometry of a fault zone containing fault segments and relay ramps. Aggregate profile is the sum of displacement of the overlapping segments. (c) Relay ramp between two normal fault segments and associated displacement profile. *Overlap* and *separation* corresponds to the length and the width of the ramp, respectively. *Relay displacement* and *overlap displacement* are the amounts of displacement at the centre of the overlap length and at segment tips, respectively. *Overlap displacement* corresponds to *overlap throw* of Huggins et al. (1995).

locations for fluids traps because of the folding and the disposition of small faulting that occurs in the ramp (Morley et al., 1990; Maerten et al., 2000).

(3) To improve the understanding of natural seismic hazards (Gupta and Scholz, 2000; Cowie and Roberts, 2001; Scholz and Gupta 2000), because many active faults exhibit slip on different segments (Jackson et al., 1982; Wesnousky, 1986; Roberts and Koukouvelas, 1996; Collier et al., 1998). The degree of fault segment linkage can modify earthquake sequences and/or create larger earthquakes than predicted because a fault array (Fig. 1b) can act as a single fault (Sieh et al., 1993; Ferrill et al., 1999; Gupta and Scholz, 2000; Cowie and Roberts, 2001). Furthermore, it has been recently suggested that the interaction and linkage between normal fault segments can increase slip rates along-strike of a fault array (Cowie and Roberts, 2001).

Many papers show that faults interact by local stress field modifications related to slip on faults (Palmer and Rice, 1972; Segall and Pollard, 1980; Pollard and Segall, 1987; Aydin and Schultz, 1990; Bürgmann et al., 1994; Willemse, 1997; Kattenhorn et al., 2000; Maerten et al., 2002), which leads to steeper displacement gradients at relay ramps (Peacock and Sanderson, 1991, 1994; Dawers and Anders, 1995; Willemse et al., 1996). Several papers suggest that fault linkage at relay ramps is governed by fault interaction processes, because overlapping produces: (1) a local increased shear stress at relay ramps (Crider and Pollard, 1998) and (2) a stress re-orientation as a function of σ_1/σ_2 principal stress ratio (Kattenhorn et al., 2000). Based on field data, Dawers and Anders (1995) and Trudgill and Cartwright (1994) show that fault linkage is favoured if distance separating the faults is relatively small compared with their length. By numerical modelling, Willemse (1997) shows that segment interaction and displacement gradient increases with increasing the fault *overlap/separation* ratio, indicating that relative position of the segment tips could be significant for the amount of fault interaction; this has also been suggested by Aydin and Schultz (1990), Gupta and Scholz (2000), Schultz (2000), Cowie and Roberts (2001) and Schultz and Fossen (2002). Because fault linkage seems closely related to fault interaction (Bürgmann et al., 1994; Crider and Pollard, 1998; Gupta and Scholz, 2000), the parameters reflecting stress distribution around faults (such as *displacement*, *length*, *overlap* and *separation*) should therefore be indicators of the degree of linkage between overlapping segments.

This paper focuses on the characterization of the geometry of un-linked and linked relay ramps using measurable parameters. However, choosing significant parameters of fault linkage requires understanding how a fault array evolves into a single linked fault. To provide a baseline dataset for comparison of fault arrays containing different relay ramp geometries, we first describe isolated faults from two exceptionally well-preserved fault outcrops. Second, we classify 39 relay ramps of centimetre to metre-scale into three types of relay geometries. Third, using the statistics of parameters from relay ramps and the comparison between fault arrays and isolated faults, we integrate the three types of relay geometries into an evolutionary model of two overlapping faults. This analysis reveals the parameters that should be used to characterize fault linkage and allows us to propose a linkage criterion. Finally, we discuss the scaling and the variability of the linkage criterion using published datasets from a wide variety of settings and scales.

2. Field examples and data acquisition

Two outcrops located in Spain, containing more than 100 faults, have been studied. The first one, Fumanyá, is located in the southern Pyrenees, and the second one, Nigüelas, is in the southwestern Betics (Fig. 2). The studied faults are of comparable scales, with outcrop traces ranging from 10's of

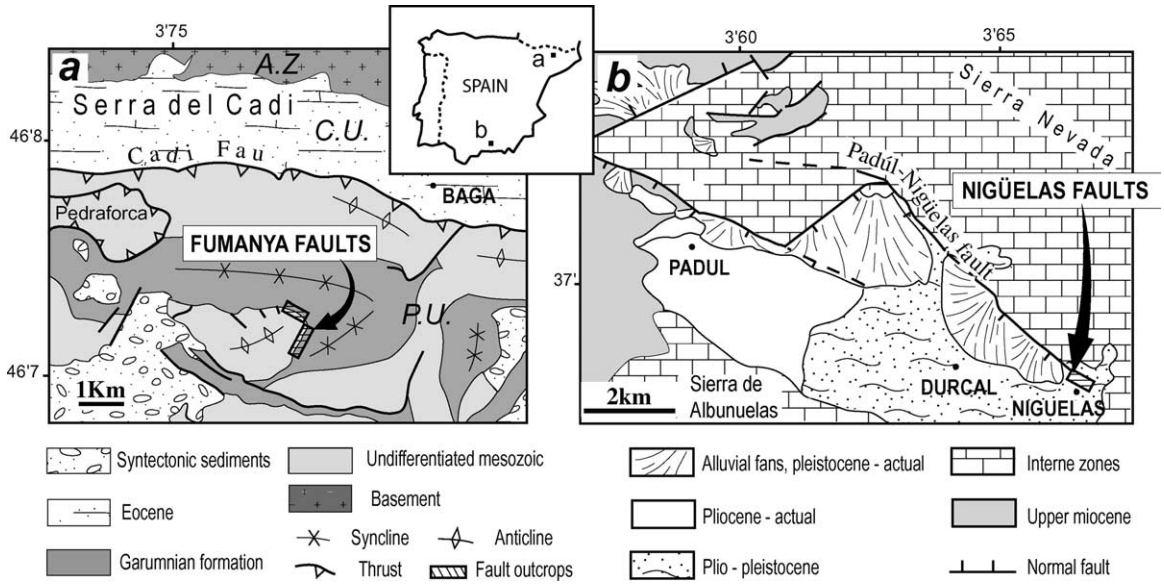

Fig. 2. Location of the study areas. (a) The Fumanyá faults (Figols Quarry, Berguedá, Catalonia), located in the Serra d'Ensije anticline, are exposed on a Maestrichtian bedding plane of the early Garumnian Formation. A.Z. = axial zone, C.U. = Cadi unit, P.U. = Pedraforca unit. (b) The Nigüelas faults (Granada province, Andalucía), located in the southwestern Betics, are exposed on a large slip surface of the Padúl–Nigüelas fault zone.

centimetres to 10's of metres and displacements from millimetres to 10's of centimetres.

2.1. The Fumanyá faults

The Fumanyá faults are exceptionally well exposed and preserved in several quarries of lignite in the 'Collado de Fumanyá' (Carbones de Berga S. A., Catalonia, Spain) (Fig. 2a). The faults are observed on a 30–70°-dipping bedding plane of a continental marly-limestone layer of early Maestrichtian age. The main exposed surface is about 250 m long by 50 m high, with more than 500 observable faults. The steep dip of this marly-limestone series results from the Pyrenean shortening during the Palaeocene–Eocene. The area is located in the ENE–WSW-trending periclinal Serra d'Ensije anticline, resulting from the interference between the E–W-trending frontal thrust and a NE–SW-striking lateral ramp of the Pedraforca thrust block (Vergés and Martinez-Rius, 1988).

The studied faults outcrop as fault scarps with normal offset of the bedding plane (Fig. 3a). The fault scarps are generally straight with an average angle of 60° between conjugate faults. Faults probably initiated during the Pyrenean orogenic folding and thrusting as normal faults. The large faults ($L > 8$ m), which displace the entire series of marls and limestone ($\sim$4.5-m-thick brittle unit), terminate in the overlying and underlying thick silty-clay layers. Longer faults (40 m) have a very high fault aspect ratio (*horizontal length/height* $= L/H \sim 8$). A detailed study of fault kinematics and slickenside morphology shows that some of these large faults ($L > 8$ m) have been reactivated with oblique slip, strike slip and rarely with a reverse component of slip, marked by striations, tensile crescentic fractures, grain crushing and sparite infilling mechanical voids. Propagated fault ends showing non-normal striations are relatively small ($\sim$1 m in the best case) and pull-apart structures indicate an amount of displacement due to oblique slip less than 10% of the scarp height. Although fault displacement due to reactivation is small, we have restricted our study to small faults ($L < 8$ m) in order to avoid the cases where linkage of segments could be favoured by oblique or strike slip. Only two studied relay ramps are between faults of $L > 8$ m, which show no evidence of reactivation, i.e. only slickenlines of normal offset (as observed on small faults).

2.2. The Nigüelas faults

The Nigüelas exposure is located in Granada Province, southern Spain, in the Padúl–Nigüelas normal fault zone, which bounds the northeastern part of the Lecrín half graben (Fig. 2b). This half graben has been related to the Neogene–Quaternary normal faulting in the Betics (Doblas and Oyarzun, 1989a,b; Alfaro et al., 2001). We have analysed a well-exposed fault system of centimetre–decimetre fault scale, called the Nigüelas fault set, containing more than 100 NE–SW striking conjugate faults. This fault set displaces an older large 35° dipping slip surface of the Padúl–Nigüelas fault (Fig. 3b) and its associated micro breccia (Doblas et al., 1997). This large gently dipping slip surface is used as a reference to measure displacement. The studied small normal faults show grooved and striated surfaces with slickenlines of normal offset and an average dip angle of 80°. The faults show no evidence of reactivation.

This work frequently refers to the displacement (net slip) distribution of faults. In both studied sites, displacement profiles were measured as scarp height versus distance along

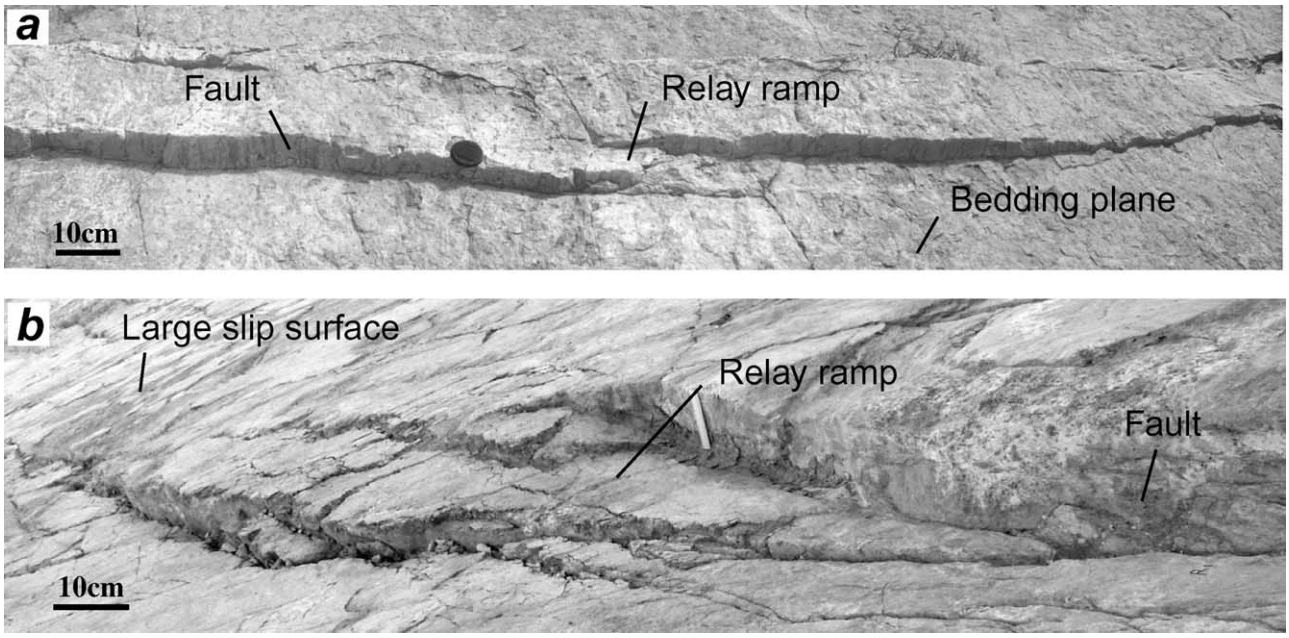

Fig. 3. Examples of faults displacing a reference surface with normal offset. (a) Fault scarps of the Fumanyá fault set displacing a limestone bedding-plane. (b) Fault scarps of the Nigüelas fault system displacing a large slip surface of the Padúl–Nigüelas fault zone. For convenience the photographs have been rotated to horizontal.

scarp. The measurement error caused by misreading is about 1 mm. The major source of error is the amount of fault scarp erosion, although the faults are exceptionally well preserved. In several cases the displacement profile of the entire fault zone has not been measured because of the large amount of erosion. For both sites, scatter related to scarp erosion is estimated at about ± 0.25 cm on average, and it never exceeds ± 2 cm on the measured fault scarps. We define D_{max} as the greatest displacement measured along a fault.

2.3. Displacement distribution of isolated faults

Displacement distribution of isolated faults has been measured and analysed in order to provide a baseline dataset for comparison of displacement profiles of segmented faults (see Section 3). The typical displacement profile of isolated faults will also be used in both fault sets as a reference to quantify and interpret the evolution of displacement distribution on segmented faults (see Section 4). An isolated fault (Fig. 1a) is defined as a fault without relay ramps showing no evidence of elastic interaction (Bürgmann et al., 1994) with surrounding faults, and which exhibits nearly symmetric displacement distribution, i.e. a 'non-interacting' fault in the terms of Gupta and Scholz (2000).

Isolated faults generally show greatest displacement at or near the centre of the fault scarp, with decreasing displacement toward the fault tips. Fig. 4 shows normalised displacement profiles of isolated faults between D_{max} and fault tips, for each studied fault set. The polynomial mean (order 4) of displacement distribution from both fault sets is nearly linear. In more detail, fault end zones show displacement gradients increasing toward fault tips and progressively decreasing toward the D_{max} position. These nearly-linear displacement profiles of isolated faults strongly resemble profiles observed on a broad range of scales by Muraoka and Kamata (1983), Walsh and Watterson (1987), Peacock and Sanderson (1991, 1994, 1996), Dawers et al. (1993), Nicol et al. (1996), Willemse et al. (1996), Cowie and Shipton (1998), and Manighetti et al. (2001).

The Fumanyá faults having length $L > 8$ m have flat-topped displacement distribution and lower D_{max}/L. This is related to the fact that they are confined within the carbonate series of 4.5 m thick, with horizontal length larger than height (fault aspect ratio $>>1$). Increase of fault aspect ratio leads typically to a decrease in D_{max}/L (Nicol et al., 1996; Willemse et al., 1996; Willemse, 1997; Schultz and Fossen, 2002), which is here expressed on displacement profile by a flat-top shape. The displacement profiles of large segmented faults at Fumanyá are also flat topped, therefore, segmented faults of $L > 8$ m have not been included in the comparison of profiles (see Sections 3 and 4).

3. Relay ramps and fault array description

Thirty-nine outcropping relay ramps of overlapping normal fault segments have been studied. The segmented faults observed on a reference surface could correspond in 3D to 'merging' (different plane at depth) or 'branching' (same fault plane at depth) faults in the terms of Willemse (1997). In several cases, especially at Nigüelas, near-tip small secondary fault traces (Fig. 3b, at the end of the rear segment) reveals a parent fault type arrangement typical of the termination of faults (Marchal, 1997; Marchal et al.,

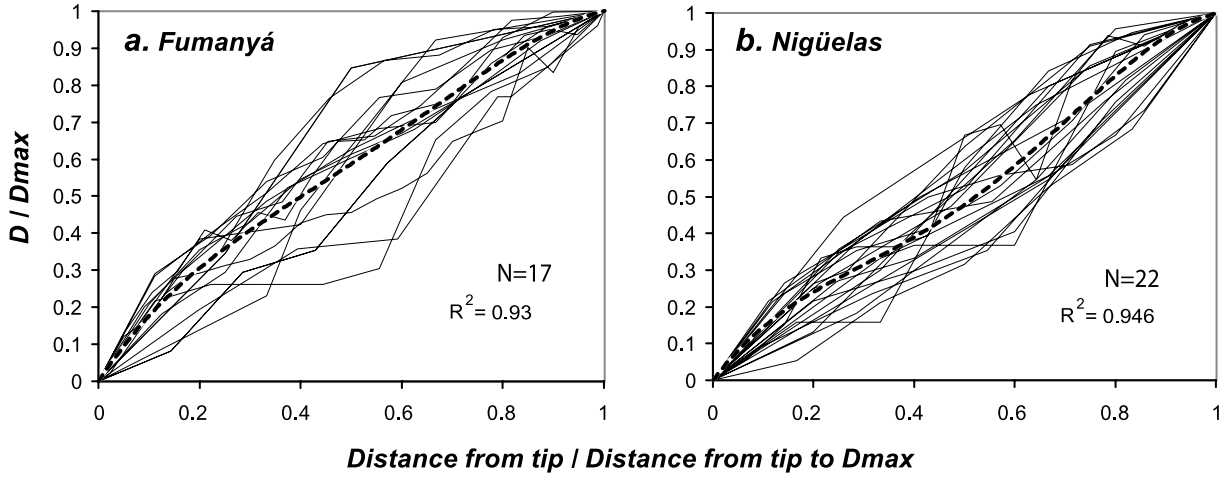

Fig. 4. Half normalized displacement profiles of isolated faults from (a) Fumanyá and (b) Nigüelas, showing nearly linear displacement distribution. Ordinate and abscissa are values of along strike *displacement* normalised to maximum displacement (D/D_{max}) and *distance from tip* normalised to *distance between* D_{max} *and tip*, respectively. Solid black lines correspond to individual fault profiles and thick broken lines are polynomial average (order 4) for which determination coefficient (R^2) is labelled. The number of half profiles (N) is also labelled in each graph. At Fumanyá only faults of $L<8$ m are presented (see text for explanations).

2003). These small secondary faults allow the formation of relay ramps of small size, interpreted as relays resulting from growing fault that breaks down into two or more small segments (merging or branching at depth).

3.1. Relay ramp terminology

Specific terminology related to relay ramp parameters used in this paper is presented in Fig. 1c. In order to analyse the evolution of linkage between fault segments, three types of geometry of relay ramps have been identified. Six examples of each type of relay ramp, which are representative of the variety of the entire population, are presented in Figs. 5–7 with associated (a) displacement profiles, (b) separation profiles, and (c) interpreted photographs. Separation profiles correspond to the distance between faults (normal to their trace) along the overlap length. 'Open relays' (Fig. 5c) are defined as overlapping parallel segments, where the relay ramp is not cut by re-orientated fault tip or through-going fractures (connecting joint or small fault). 'Linked relays' (Fig. 6c) are defined as overlapping segments where the two fault segments are incipiently linked, with little or no displacement at the branch points. Linking may occur either by curved fault tips (see relay F5), one or more through-going fractures (see relays F7 and F9), or both (see relays F1, N2 and N3). 'Fully breached relays' (Fig. 7c) are defined as overlapping fault segments, fully linked by one or both reoriented fault segment tips, and/or well developed through-going faults. In this case, displacement has to be well developed at the branch points, i.e. over 20% of the average aggregate displacement of the overlap zone (Figs. 5–7).

3.2. Open relays

Eleven open relays have been recorded. Fig. 8a presents displacement profiles of five fault arrays containing open relays between two overlapping fault segments. In Fig. 8, all segment arrays constituted by more than two fault segments were on purpose excluded in order to properly compare similar segmentation features, and especially avoid the case of multiple segment array showing different relay types. This explains why less fault arrays are presented in Fig. 8 compared with the amount of studied relays (here 11 open relays). The profiles of Fig. 8a reveal a mean zone of minimum displacement at overlap, which is between individual D_{max}, each one approximately located at the centre of each fault segment. The displacement distribution of the fault array is compared with the displacement profile of an 'ideal isolated fault' of the same length, constructed for each fault set with both polynomial mean distribution of Fig. 4 and the least square value of D_{max}/L. Displacement profile of the entire fault array is 'incoherent' (different displacement geometry) with the displacement distribution of an ideal isolated fault (Fig. 8a). Almost all segments from open relays exhibit nearly symmetric displacement profiles consistent with displacement distribution and D_{max}/L values of isolated faults.

Overlap zone displacement and separation profiles of six representative examples of open relays are presented in Fig. 5a and b. Displacement distribution of aggregate profiles (broken lines in overlap zones) exhibits a characteristic irregular shape at relay ramps (Fig. 5a). In more detail, especially on relays from Fumanyá, aggregate profiles exhibit local displacement excess between minima values located at the vicinity of the segment tips. This reflects the non-linear end shapes of the displacement distribution observed on each fault segment. Fig. 9 allows us to compare *overlap displacement* to *overlap* ratio (approximately equivalent to displacement gradient within non-breached relay ramps; see Fig. 1c) to displacement

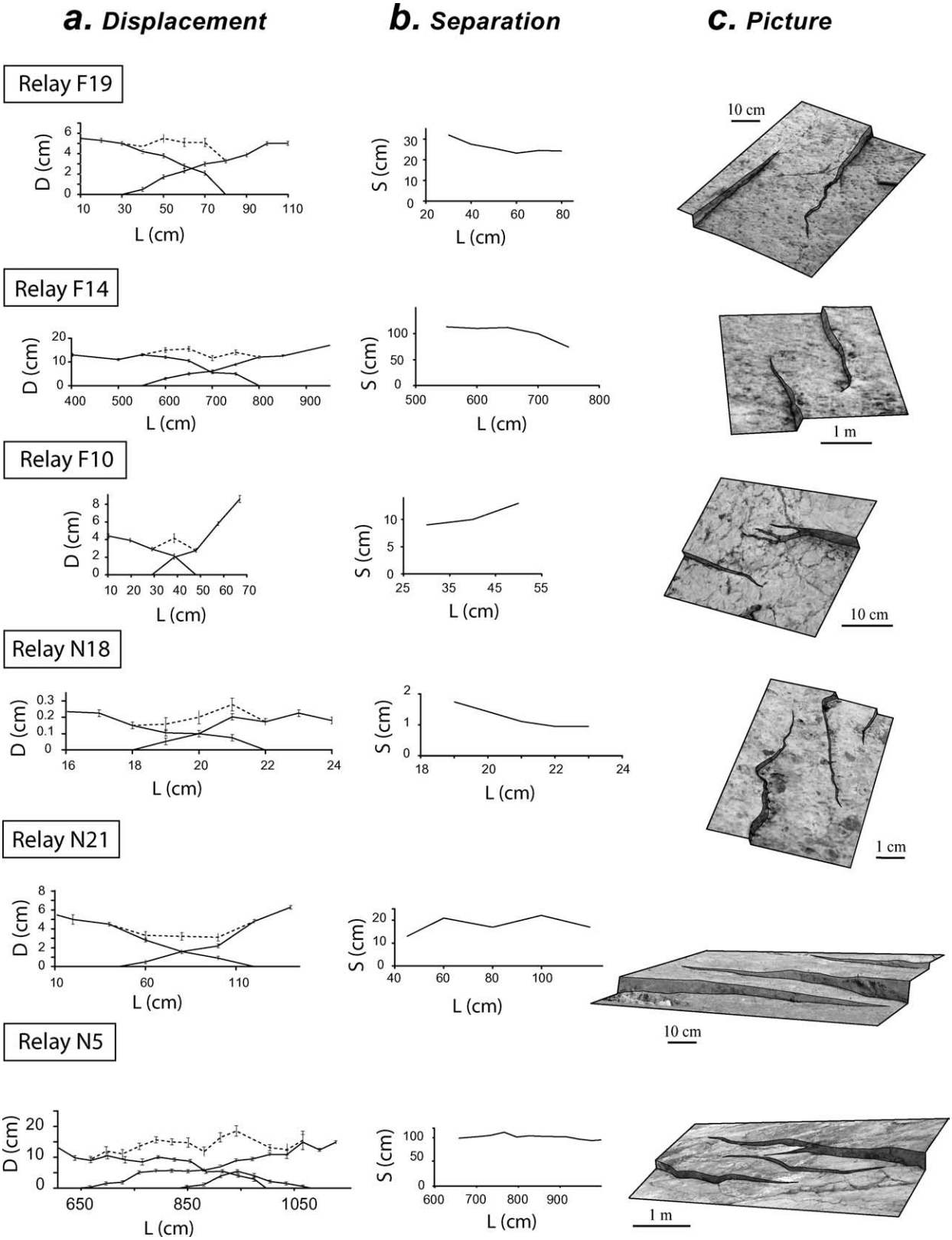

Fig. 5. Examples of open relays. (a) Displacement profiles at relay ramps, (b) associated separation profiles (distance between faults normal to their trace along overlap), and (c) rendered photograph of each relay. Relays referenced by the letters F and N are from Fumanyá and Nigüelas fault sets, respectively. In displacement profiles, broken lines represent aggregate profiles at the overlap zone. Displacement profiles of each segment are projected following an axis perpendicular to fault segments. Error bars are labelled on profiles. Separation is taken following an axis perpendicular to fault segments, and error is about 1 mm.

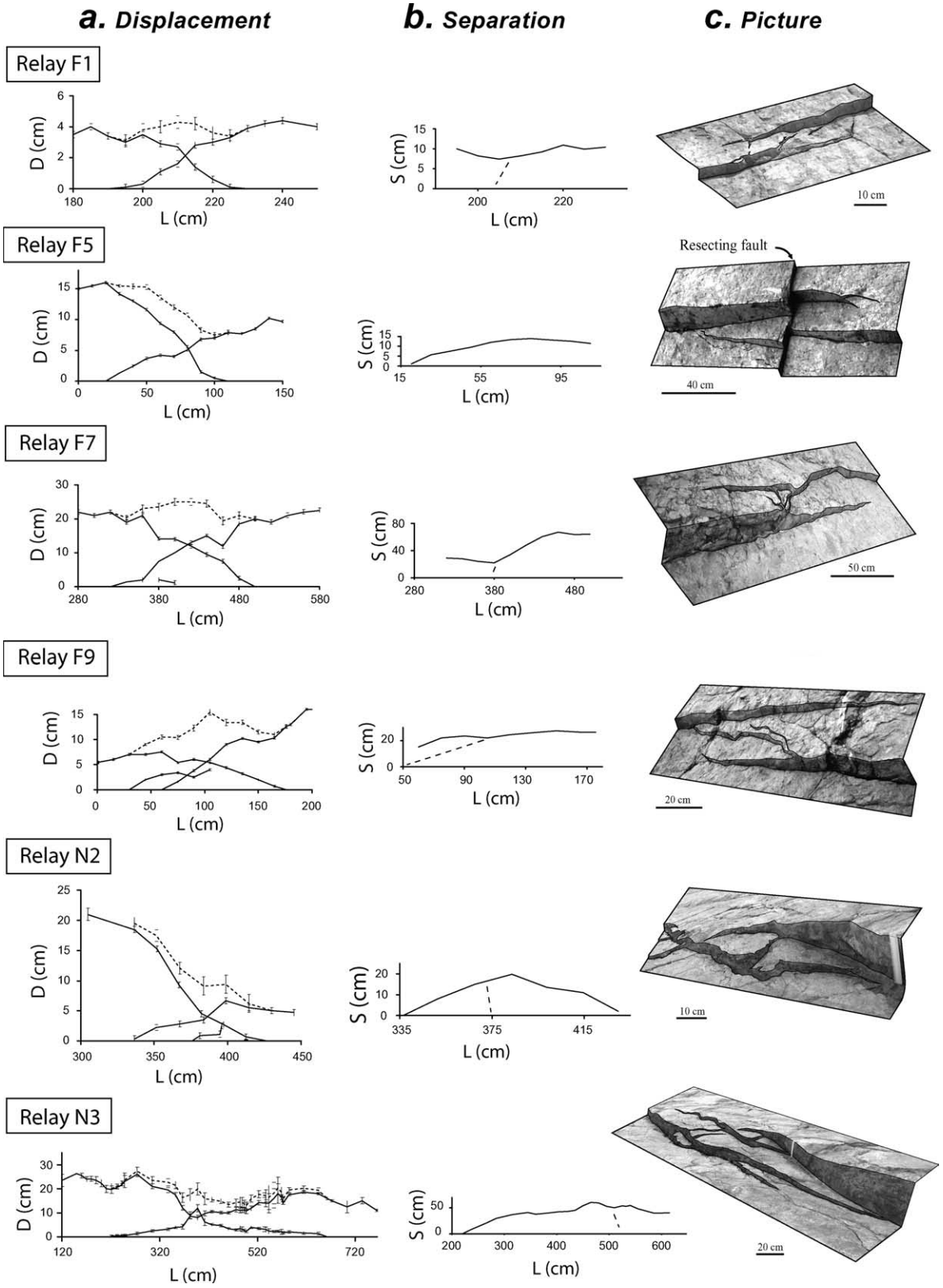

Fig. 6. Examples of linked relays; see text of Fig. 5 for more details. In separation profiles (b) broken lines represent linking through-going faults.

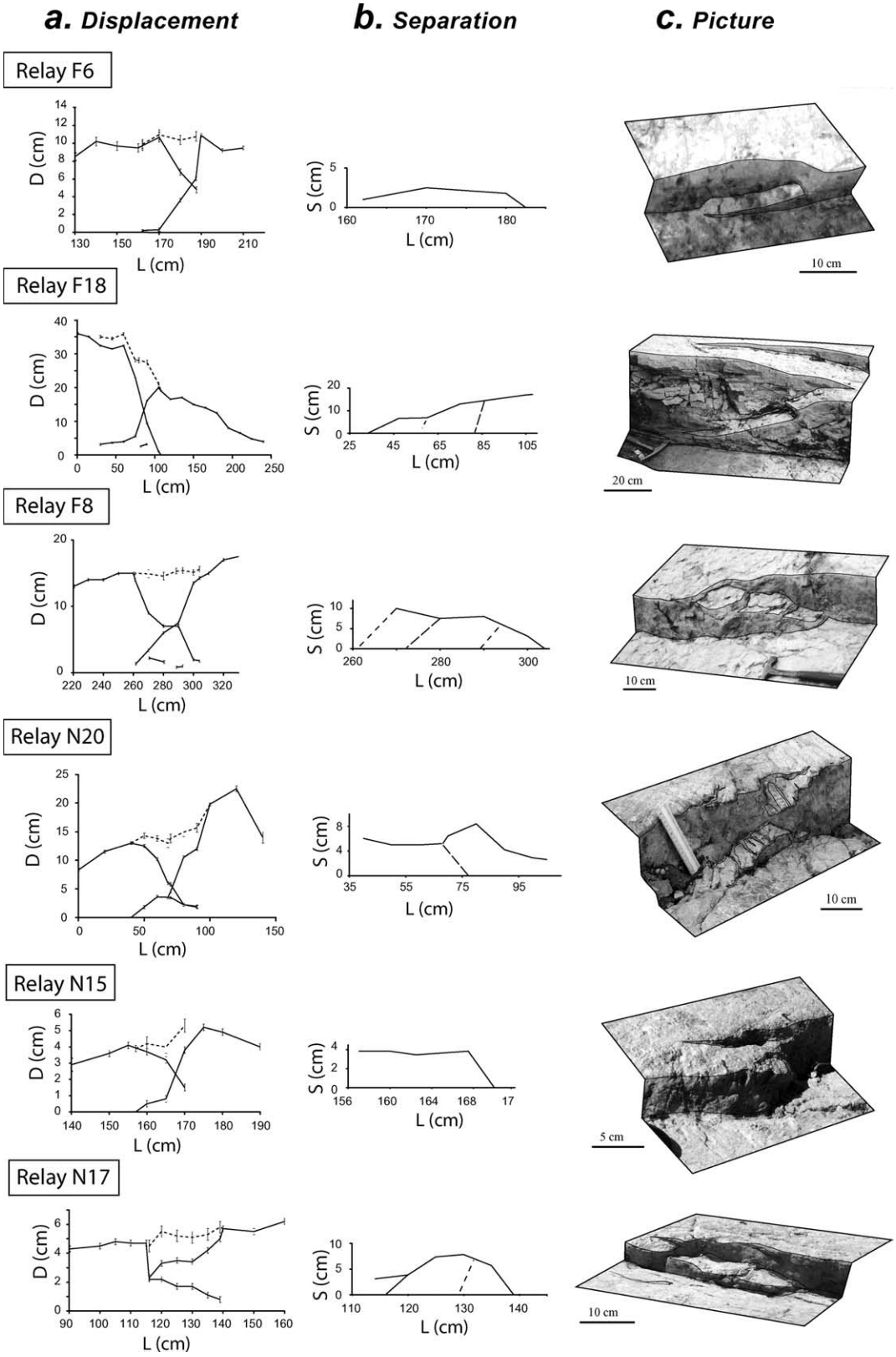

Fig. 7. Examples of fully breached relays; see text of Figs. 5 and 6 for more details.

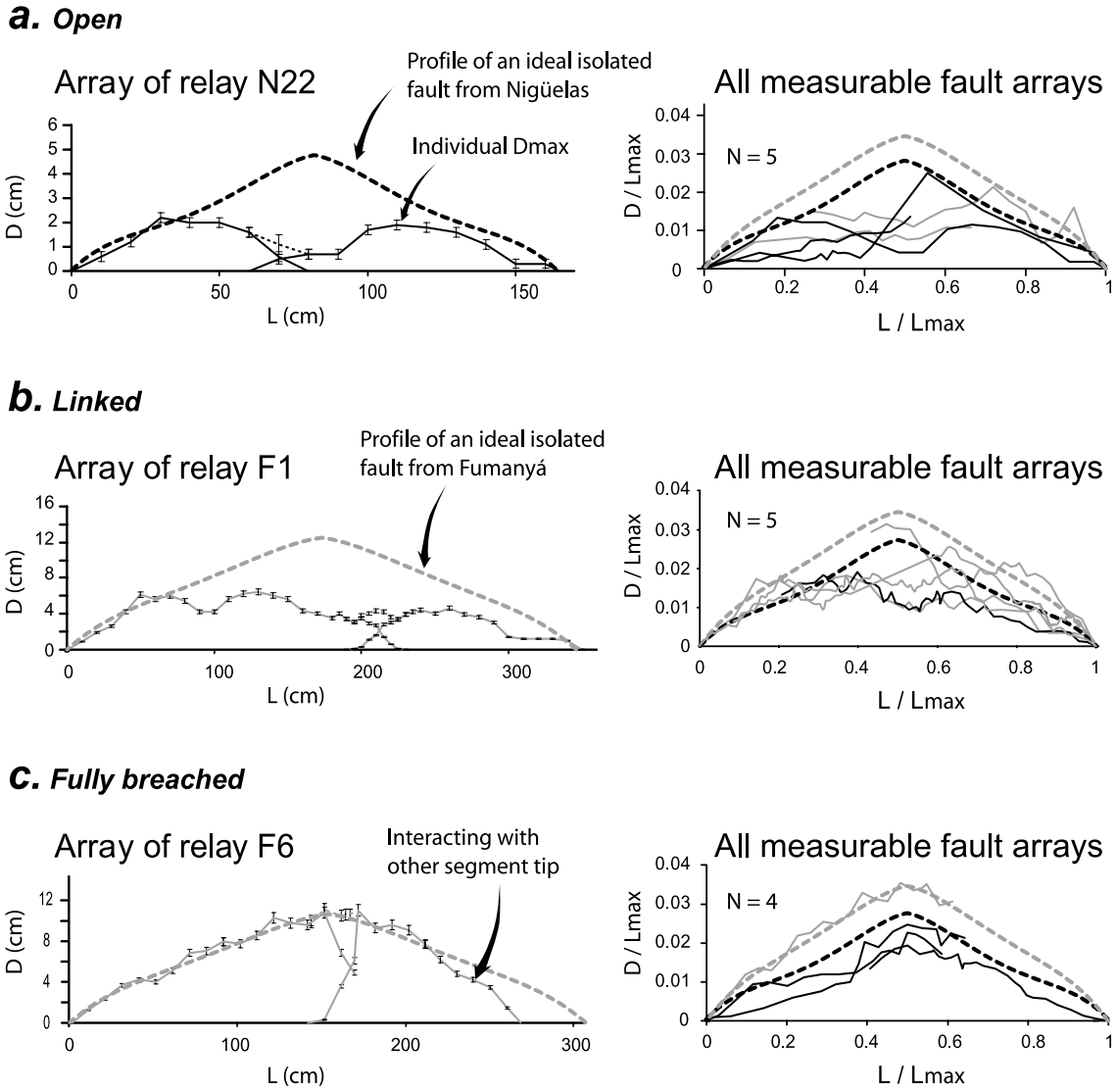

Fig. 8. Displacement distribution of fault arrays containing two overlapping fault segments having (a) open relays, (b) linked relays and (c) fully breached relays. Displacement profiles of one example of fault array (with reference labelled, N22, F1 and F6) and normalised aggregate profiles (D/L_{max} vs. L/L_{max}) of all measurable fault arrays are shown. Solid grey lines and solid black lines are for Fumanyá and Nigüelas faults, respectively. On examples N22, F1 and F6, aggregate profiles are represented by small broken lines at overlap zones. Thick broken grey and black lines are the profiles of ideal isolated faults from Fumanyá and Nigüelas, respectively (see Section 3.2 for explanations). The displacement profile is not entirely shown when the fault scarp is not well preserved or when the entire fault array does not outcrop. For the special case of the array of the relay F6, the profile of the array is shown, whereas one segment interacts with another not linked fault. In this case, as for the case where the fault does not entirely outcrop, the normalized profile is adjusted positioning D_{max} at $L/L_{max}=0.5$.

gradient of isolated faults for each type of studied relay. These data reveal that values of mean displacement gradient are on average near those of isolated faults, although they are slightly higher at Fumanyá (with a larger standard deviation) and slightly lower at Nigüelas. Fig. 10a presents the different studied relays with respect to their *overlap* and *separation*. These parameters defined in Fig. 1c are taken using the separation profiles of Fig. 5b. This representation (Fig. 10a) displays the geometric relay variability, in which open relays exhibit low relay aspect ratio (*overlap*/*separation*) compared with linked and fully breached relays.

3.3. Linked relays

Ten linked relays were analysed, and displacement profiles of five fault arrays containing linked relays between two overlapping fault segments are presented in Fig. 8b. The displacement distribution is incoherent with the displacement distribution of an ideal isolated fault having length equal to the entire fault array. Relay ramps exhibit zones of displacement minima, and each segment shows individual D_{max} with an asymmetric displacement distribution with respect to displacement gradients at fault ends.

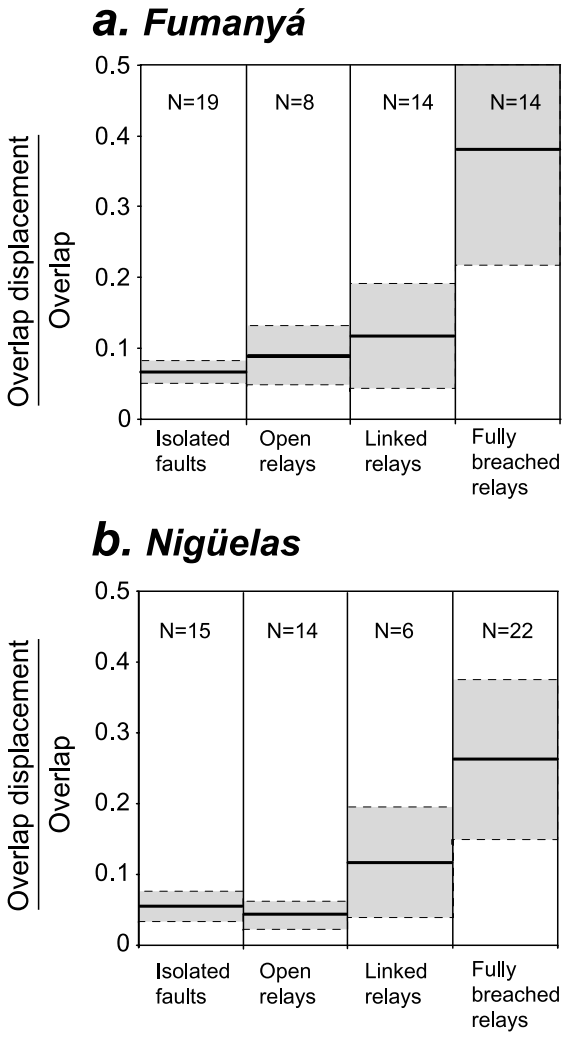

Fig. 9. Histograms of *overlap displacement* to *overlap* ratio for different types of relay ramps from (a) Fumanyá and (b) Nigüelas. Also shown are data for isolated faults, for which the ordinate axis represents values of $2D_{max}/L$. Black lines represent mean values and shaded area is plus and minus standard deviation. *Overlap displacement* (see Fig. 1c) corresponds to the amount of displacement at the end of the ramp. *Overlap displacement* to *overlap* ratio is therefore an approximation of displacement gradient of a segment at relay ramp only for open and linked relays.

Six representative examples of displacement and associated separation profiles of linked relays are presented in Fig. 6. Zones of linkage are represented on separation profiles by broken lines (for zones of through-going faults) and by minima at the ramp ends (for the zones of segment tip connections). Displacement distribution of aggregate profiles (Fig. 6a) presents an irregular shape. In further detail, at the location of the linkage by a segment tip, aggregate profiles exhibit well-developed displacement (see relays F5, F7, F9 and N2), i.e. there is no displacement minimum as frequently observed at ramp ends where there is no linking fault (see F5 and F9). Also clearly observed are high segment displacement gradients in overlap zones compared with gradients around the relay. This can also be observed in Fig. 9, which reveals that mean values of *overlap displacement* to *overlap* ratios in linked relays are higher than in open relays and isolated faults, but of comparable mean values (around 0.12) and standard deviation in both fault sets. Displacement profiles of the relay ramps in Fig. 6a can be quite symmetric (see relays F1 and F7) or very asymmetric (see relays F5 and N2). The asymmetry in displacement gradient is the source of the large standard deviation of *overlap displacement* to *overlap* ratios (Fig. 9). On map view, the values of relay aspect ratios (*overlap*/*separation*; Fig. 10a) are scattered and, on average, relatively higher than for open relays.

3.4. Fully breached relays

Eighteen fully breached relays have been studied. Displacement and separation profiles of six representative examples of fully breached relays are presented in Fig. 7. The fault segments are well connected by through-going ramp faults and/or by reoriented segment tips. Connecting geometry can be by a single plane (relays F6, N15) or more complex (relays F18, F8, N17 and N20) with multiple linking faults. Values of D_{max}/L and displacement distribution of the entire fault array constituted by two fully breached fault segments are near those of an ideal isolated fault, although with lower values of displacement in many cases (Fig. 8c). Aggregate profiles generally show continuous displacement shapes with fault profiles around the relay ramp (Fig. 7a). Relay ramps do not exhibit large displacement irregularity although displacement is lacking when the dip of the relay ramp toward the hanging wall is large (about 30° for the relay N20) (see also Huggins et al., 1995).

The high values of *overlap displacement* to *overlap* ratios observed in Fig. 9 show that fully breached relays accommodate a large part of displacement compared with open and linked relays. This is also exhibited on displacement profiles (Fig. 7a) by: (1) the amount of displacement at branch points, and (2) high displacement gradients with their steep accentuation in overlap zones. Fig. 10a reveals that *overlap*/*separation* values of fully breached relays are very scattered, but are on average the highest of the three relay ramp types.

4. Fault interaction and linkage

In this section we discuss the evolution of displacement profiles and relay geometry during the linkage process using: (1) the quantitative comparison of the displacement profile of fault segment arrays with regard to an ideal isolated fault, and (2) the statistics of relay ramps parameters. This will allow us to integrate the three types of relay ramp geometries into the evolution of fault linkage, to identify the main parameters controlling the initiation of linkage, and then to propose a linkage criterion.

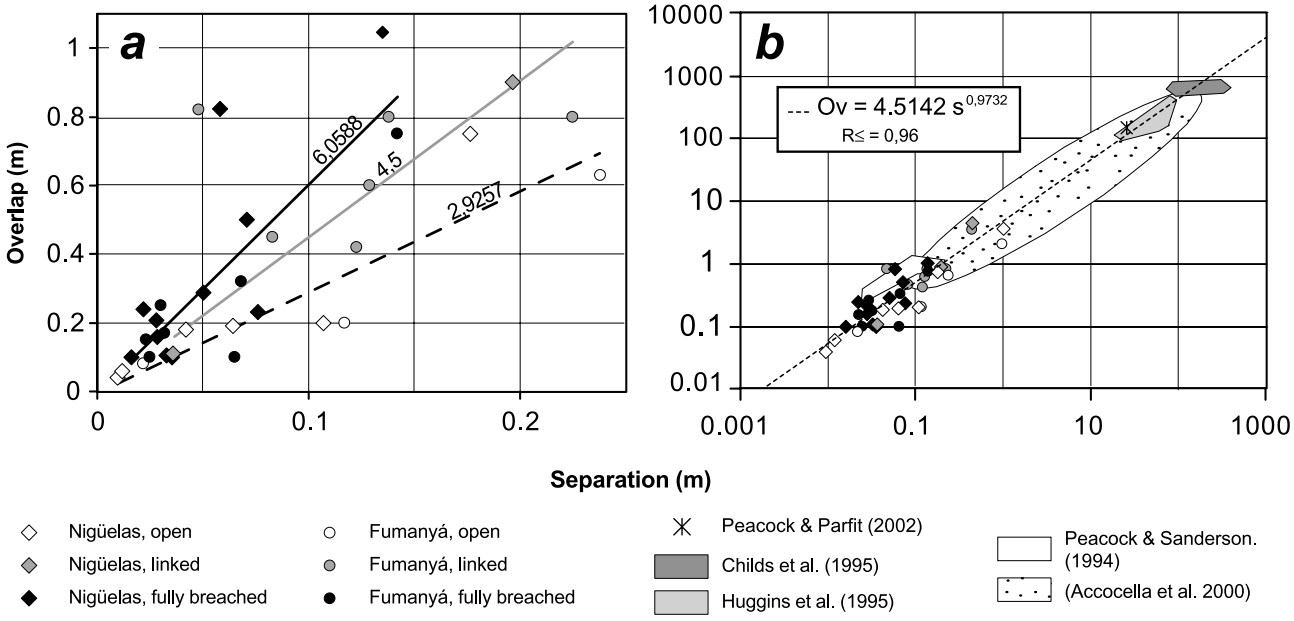

Fig. 10. (a) Graph of *overlap* (*O*) vs. *separation* (*S*) of relay ramps from Fumanyá (circles) and Nigüelas (squares). Values of separation are taken at the centre of the overlap zone. The broken line is the best-fit linear trend for open relays dataset, the solid grey line for linked and the solid black line for fully breached relays, with gradient values labelled. For convenience of legibility, four relays of nearly-metric scale are not represented in this graph, but are plotted on (b). (b) The same data on a bi-logarithmic graph, also including other published datasets over a large scale-range. The broken line is the best-fit power law trend, presented with equation and determination coefficient (R^2).

4.1. Open relay formation

The difference of displacement profile shape between fault arrays and an ideal isolated fault can be quantified by measuring and comparing the areas under the profiles of Fig. 8. The area under the aggregate profile of each fault array containing open relays ranges between 33 and 59% of the area under the profile of an ideal isolated fault of equivalent length (Fig. 8a). In contrast, displacement profile shape of each fault segment is only slightly different from the profile of an ideal isolated fault. The similarity between individual fault segments and ideal isolated faults suggests that open relays result from the lateral propagation of underlapped faults (see Fig. 14 in Gupta and Scholz, 2000; note that in their model the faults show no overlap).

Anomalies of displacement gradients at overlap zones are used as an indicator of fault mechanical interaction (Willemse et al., 1996; Crider and Pollard, 1998; Gupta and Scholz, 2000). The fact that displacement gradients at relay ramps are near those of isolated faults (Fig. 9) suggests that interaction, if any, was weak during the first step of the relay ramp development. This is probably related to the specific near tip stress distribution of the studied faults during their activity.

4.2. Linkage

The area under the aggregate profile of each fault array containing linked relays ranges between 54 and 84% of the area under the profile of an isolated fault of equivalent length (Fig. 8b). As Peacock and Sanderson (1991) and Trudgill and Cartwright (1994) did, we interpret the linkage observed on the plane of inspection as the evolution of the propagation of fault segments from open relays. The comparison of profile shapes of fault arrays containing open and linked relays (Fig. 8a and b) suggests that displacement was redistributed along the whole fault array. The higher *overlap/separation* ratio for linked relays than for open relays is consistent with a more evolved stage in fault overlap and linkage. The low values of separation at segment tips (relays F5, N2 and N3 of Fig. 6b) and the presence of through-going faults at relay ramps (relays F1, F7, F9, N2 and N3), indicate that fault tips and/or through-going faults propagated through the relay ramp. In Section 3.3 we have observed that: (1) displacement is well developed around the locations of segment tip linkage and through-going faults, and (2) displacement gradients increase at relay ramps (see the difference between open and linked relays in Fig. 9). This provides evidence that linkage initiation favours the displacement accumulation and redistribution at relay ramps, although displacement deficit still occurs.

Steep overlap displacement gradient at relay zones (Figs. 6a and 9) indicates that strong interaction occurred during this stage of linkage (see Peacock and Sanderson, 1991; Dawers and Anders, 1995; Willemse et al., 1996). Initiation of linkage and fault interaction (i.e. the formation of linked relays) can be expressed with respect to the relay aspect ratio. Although data are spread out, Fig. 10a shows, on average, that for a given low value of separation, fault

linkage is reached with low values of overlap. This indicates that fault interaction and linkage initiation occur earlier during fault overlap for small values of separation than large.

4.3. Full breaching

A fundamental problem arises in interpreting some fully breached relays from the evolution of open and linked geometries. Fully breached geometries showing tip connections (see Fig. 7c, relays F6 and N15) could also be interpreted as fault bifurcation into two branches, during its propagation along strike, leading to an apparent fully breached relay (see Childs et al., 1996). In order to avoid misinterpretation we only present fully breached relays showing: (1) high displacement gradient at the overlap zone, (2) 'hook' shapes (see relay F6, F8, N15 and N17 of Fig. 7c), and not 'Y' shape on map view (feature of fault bifurcation; Childs et al., 1996), or parallel faults linked by an oblique or perpendicular through-going fault at relay ramp (see relay F18 and N20).

The area under the aggregate profile of each fault array containing fully breached relays ranges between 69 and 99.3% of the area under the profile of an ideal isolated fault of equivalent length (Fig. 8c). The comparison of displacement profiles of Fig. 8b and c suggests that during full breaching, displacement accumulated and was redistributed along the entire fault array, so that the displacement profile evolves towards the 'nearly-coherent' profile with an ideal isolated fault. The term 'nearly-coherent' is used because the fault profile could be 'under displaced' (Fig. 8c) if, for example, fault activity stops before its entire displacement readjustment. Therefore, after linkage, displacement has been principally added on linked fault planes, as suggested by the displacement observed at branch points of fully breached relays.

The dataset in Fig. 10a shows that full breaching is mainly observed for values of separation less than 0.1 m, and over a value of relay aspect ratio (*overlap*/*separation*) ~6. This suggests that: (1) fault separation controls fault's ability to link, and (2) fault overlap could continue during the period of full breaching of the fault segments.

As proposed by Peacock and Sanderson (1991) and Trudgill and Cartwright (1994) the three types of relay can be integrated in a continuous evolutionary model in which fault interaction leads to fault linkage. We have quantitatively shown that fault displacement profile, displacement gradient at a relay ramp, and relay aspect ratio are significant to the evolution of fault linkage and may be used to establish a linkage criterion for segmented normal faults.

5. Segment linkage criterion

Separation and *overlap*, the geometrical parameters used to represent relay scaling and fault segment interaction are easy to obtain on map views (Aydin and Nur, 1982; Aydin and Schultz, 1990; Huggins et al., 1995; Accocella et al., 2000). These parameters in their simple form do not allow discrimination between the different relay geometries. Gupta and Scholz (2000) propose that *overlap* and *separation* should be normalised to a fault segment length, in order to consider fault stress perturbation around a fault segment. They show that the amount of interaction is a function of the relative fault tip position with the stress drop around fault, and therefore a function of the *separation* with the collateral fault segment. However, the utilization of the *segment length* reveals a problem for the representation of fully breached relays. Physically linked segments (i.e. no longer interacting) should not be represented with a linkage criterion that uses *segment length* because the array could have propagated after linkage. We choose therefore to focus on parameters of the relay ramp because: (1) they can be used in arrays of multiple fault segments where lengths of central segments should not be taken, (2) they can be measured even if the entire fault array cannot be observed, and (3) fully breached relays can be represented.

5.1. Relay displacement (D)–separation (S) diagram

We propose a *relay displacement–separation* diagram to define the segment linkage criterion considering that the amount of displacement at relay ramp (Fig. 9) (e.g. Trudgill and Cartwright, 1994; Contreras et al., 2000; Mansfield and Cartwright, 2001) and fault *separation* (Fig. 10a) (Willemse, 1997; Gupta and Scholz, 2000) control the fault's ability to link during overlap (see Section 4).

Relay displacement (*D*), which is the sum of displacements of each fault segment, and fault segment *separation*(*S*) (Fig. 1c) are measured on the relay ramp on a line normal to the ramp strike at the centre of the overlap length. The results are presented in Fig. 11a and b for the Fumanyá and the Nigüelas sites, respectively. On the graphs, the three different relay types are distinguished by different symbols. Open relays exhibit low values of c ($c = D/S$), less than 0.53 and 0.31 at Fumanyá and Nigüelas, respectively (except for a relay of very small scale at Fumanyá). Linked relays show higher values of c, with $0.53 < c < 1.2$ and $0.31 < c < 0.6$ at Fumanyá and Nigüelas, respectively. Fully breached relays exhibit the highest values of c, always over 1.2 and 0.6 at Fumanyá and Nigüelas, respectively.

Referring to Section 4, linked relays reflect the initiation of fault linkage during their overlap. Hence, the diagram fields of linked relays (grey areas) are zones within which the faults link when *relay displacement* increases during fault segment overlap. We define a '*linkage threshold*' as the best-fit linear trend of linked relays ($D = c^*S$; Fig. 11a and b), having a slope of *linkage threshold* (c^*) of 0.6 and 0.34 for the Fumanyá and the Nigüelas fault sets, respectively. Note that least square determination coefficient (R^2) is not significant for the Nigüelas fault set because of the low number of linked relays. Displacement gradients

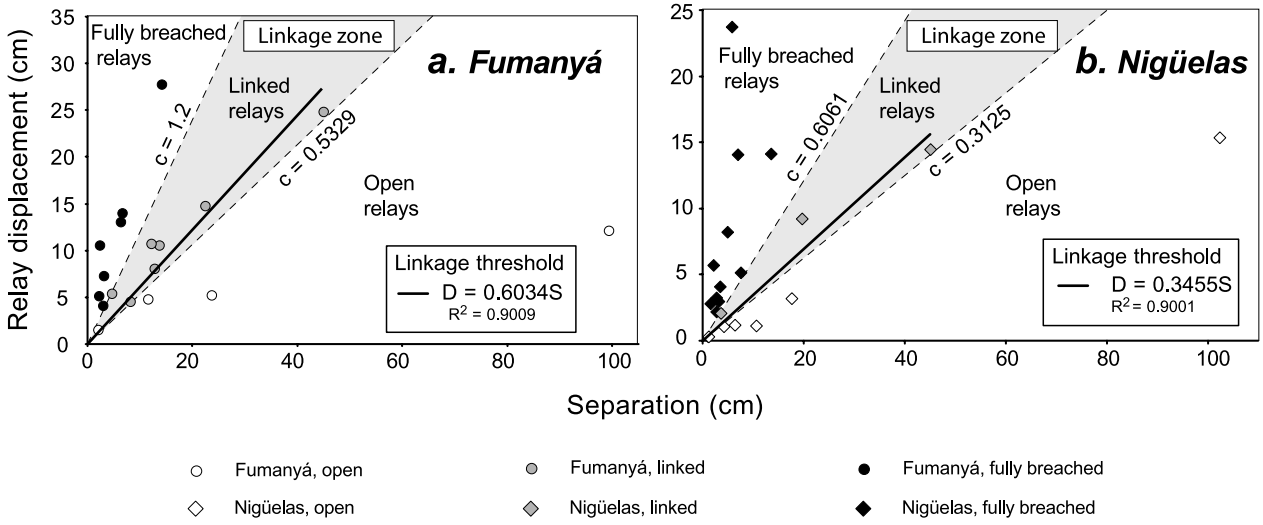

Fig. 11. Graphs of *relay displacement* (*D*) vs. *separation* (*S*) of the different types of studied relays from (a) Fumanyá and (b) Nigüelas. Shading represents fields including the linked relays, bounded by specific values of $c = D/S$. Bold lines, defined as *linkage thresholds* ($D = c*S$), are the best-fit linear trends of linked relays, for which equations and determination coefficients are labelled.

at overlap zones (Figs. 5a, 6a, 7a, and 9) show that open and linked relays are closely related to the relative amount of interaction between faults. Thus, this system of representation (*D* vs. *S*) also allows the distinguishing of: (1) weakly interacting, (2) highly interacting and (3) fully breached segments of Fumanyá and Nigüelas fault sets.

5.2. Published datasets from a broad range of scales on the D–S diagram

We show in Section 2.3, that displacement geometry of isolated faults from Fumanyá and Nigüelas (Fig. 4) reveals similar displacement distribution with faults of large scale. In addition, all relay ramps compiled in Fig. 10b (from Peacock and Sanderson, 1994; Childs et al., 1995; Huggins et al., 1995; Accocella et al., 2000; Peacock and Parfitt, 2002, including this study) exhibit nearly linear relation (power law with exponent $n = 0.97$), which indicates self-similar relay geometry (i.e. similar *overlap/separation* ratio, about 4.5) on a broad range of scale. This suggests that the linkage criterion could also be observed on segmented faults of large scale.

To test the scalar validity of our linkage criterion, we present both the studied relays and the relay ramps from the literature on a bi-log *relay displacement–separation* diagram (Fig. 12). Only relays published with displacement profiles and map views with precise scale, on which relay drawings or aerial photographs are of enough quality to characterise their geometry accurately (see references on

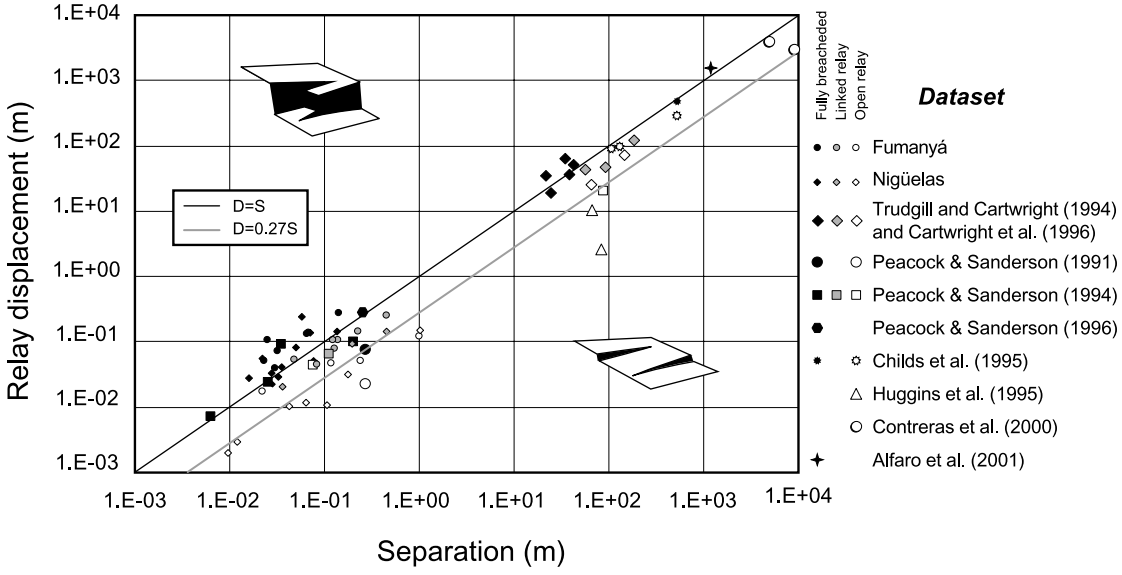

Fig. 12. Bi-logarithmic graph of *relay displacement* vs. *separation* including both the studied dataset and other published datasets over a large scale-range (see text for explanation). The grey straight line is the maximum value of *relay displacement* to *separation* ratio ($c = D/S$) for the data composed only of open relays, with equation labelled. The black straight line is the minimum value of *c* for the data composed of fully breached relay, with equation labelled.

Fig. 12), have been plotted. Fig. 12 shows that there is no significant difference in values of c between relays of small scale (separation about 0.01 and 1 m) and large scale (100–1000 m). Open relays exhibit low values of c (frequently lower than 0.3), fully breached relays show high values (frequently over 0.8), and linked relays when they can be identified (see aerial photographs and drawings in Trudgill and Cartwright (1994) and Cartwright et al. (1996)) are of intermediate values between open and fully breached. The straight grey line, with $c=0.27$, represented in this diagram limits the field composed only of open relays. The straight black line, with $c=1$, limits the field only composed of fully breached relays (except for one linked relay from the Fumanyá site). The field located between these two lines, which includes linked relays, is the range of natural variability in slope of the *linkage threshold* (c^*) (see Section 6).

Datasets having the three relay types defined in this study exhibit different values of c^* within a range that does not span over one order of magnitude ($0.27<c^*<1$). For the Fumanyá and the Nigüelas fault sets c^* is 0.6 and 0.34, respectively (Fig. 11). At Canyonlands, c^* is 0.65 for relays from Trudgill and Cartwright (1994) and Cartwright et al. (1996). For the dataset of Childs et al. (1995) c^* is estimated at 0.91. Several relays from the dataset from Somerset (England) described by Peacock and Sanderson (1991, 1994, 1996) do not exhibit a good sorting, whereas other relays in their data match the overall sorting. We conclude that a bi-log *relay displacement–separation* diagram allows fields of relay ramp geometry to be identified: relays having $c<0.27$ are open, and those having $c>1$ are fully breached.

6. Discussion: linkage variability, scaling and relay geometry prediction

This section focuses on two main points. First, we discuss the variability in linkage threshold and the potential sources of anomalous relay geometry with the presented linkage criterion. Second, we discuss the scaling of the linkage criterion and its implication for predicting relay types.

6.1. Source of linkage variability

The origin of linkage threshold variability does not seem simple. We can invoke different sources that can be specific to a fault system as the typical displacement distribution of faults, or to a local array, as fault geometry at depth and local host rock heterogeneity.

6.1.1. Displacement distribution at relay ramps

In both studied fault sets, linkage occurs for similar values of *overlap displacement* to *overlap* (Fig. 9) and relay aspect ratios (Fig. 10a). This indicates that the difference observed in slope of linkage threshold ($c^*=0.6$ and 0.34 at Fumanyá and Nigüelas, respectively) is mainly due to the shape of the displacement profile at relay ramps, which is quite different between the two studied fault sets. Figs. 5a and 6a show that the displacement profiles in overlap zones of open and linked relays are commonly linear or concave upward at Nigüelas, even though they are commonly convex upward and rarely linear at Fumanyá. Differences in displacement distribution of relay ramps at the initiation of linkage could also be responsible for the *linkage threshold* variability observed in Fig. 12. Note that displacement profiles at overlap zones of the published datasets of Fig. 12 (Peacock and Sanderson, 1994; Childs et al., 1995; Huggins et al., 1995; Accocella et al., 2000) also reveals different shapes, principally linear and convex upward.

Different displacement distribution between Fumanyá and Nigüelas fault sets is observed in open relays (Fig. 5a), linked relays (Fig. 6a), and also in the displacement profiles of isolated faults (Fig. 4). Using the average displacement profiles of isolated faults and the typical values of D_{max}/l, the displacement along Fumanyá isolated faults can be estimated in the best case to 1.4 times per unit length the displacement at Nigüelas. This factor does not explain the entire difference observed between *linkage thresholds*, which is about a factor of two (Fig. 11). This suggests that other processes could favour this difference of *linkage threshold*.

6.1.2. Linkage during interaction

By numerical modelling, Crider and Pollard (1998) show that decreasing fault aspect ratio (L/H) (i.e. increasing fault height) leads to an increase in the ability of the faults to link at the relay ramp, because of the large superposition of high shear stress. This is justified because horizontal displacement gradient increases with the decrease of fault aspect ratio (relative increase of fault height; see Willemse (1997) and Schultz and Fossen (2002)). The differences in fault aspect should have a low effect on the linkage criterion ($D=c^*S$), which integrates the amount of displacement. Willemse (1997) shows that the size of the cohesive end zone can also influence the fault's ability to interact. Variation in the size of the cohesive end zone, which is explicitly related to the driving stress of the fault and the yield strength of rock surrounding the fault (Schultz and Fossen, 2002), could therefore be responsible for part of the scatter of the *linkage threshold* in Fig. 12. Another source of difference in linkage initiation is the ramp strength related to local extension produced at ramp cut-offs. Ferrill and Morris (2001) show how cut-off elongation should evolve with the increase of displacement gradient related to fault interaction. This suggests that for a given elongation, brittle rocks of low shear strength should favour relay ramp linkage than sediments of plastic behaviour.

6.1.3. Branching and merging fault geometries

Relay ramps presented in Fig. 12 are not sorted according to their geometry at depth, 'branching' and 'merging' in the terms of Willemse (1997). Huggins et al. (1995) show that

in each case ('branching' or 'merging') fault growth can lead to strike overlap, interaction and linkage. Walsh et al. (2003) suggest that displacement profiles of 'branching' and 'merging' faults are quite different, which could constitute a source of the linkage variability observed in Fig. 12. Peacock and Parfitt (2002) show with analogue models that undulated morphology at depth leads to apparent underlapping cracks with 'through-going fractures' extending from near the tips. In the datasets of Fig. 12 only overlapping fault segments are included.

6.1.4. Local heterogeneity

Local heterogeneous elastic properties or local variation in fault height could account for anomalous relay type within a single dataset. Cowie and Shipton (1998) show how fault end zones are sensitive to local heterogeneity. This suggests that fault linkage between fault tips could for example be locally enhanced or inhibited by a local reduction or increase in relay ramp shear strength, if the relay ramp is constituted by a lithology different from that of the overall rocks.

6.2. Linkage scaling and its implications for predicting relay geometries

Although many works present well-exposed relay ramps, particularly in normal fault systems, few published works exhibit both relay ramp displacement profiles and accurate map views on which fault *separation* can be measured. This accounts for the limited number of included published data and the lack in values for relays of metre-scale (1–10 m in *separation* and *relay displacement*). However, this dataset suggests that a *linkage threshold* ($D = c^*S$) should control strike linkage of overlapping fault segments on a broad range of scale. On Fig. 12, scatter in slope of *linkage threshold* does not span over one order of magnitude ($0.27 < c^* < 1$). *Relay displacement* and *separation* are self-similar at linkage over a large scale-range, which suggests that fault strike linkage is governed by similar fault interaction from centimetre- to kilometre-scale.

The observed small variability in *linkage threshold* suggests that natural relay geometries of normal fault could be predicted using *relay displacement–separation* diagrams. We address the term 'prediction' to the identification of relay geometry (open or fully breached): (1) at earth surface, where erosion or syntectonic deposit catchments affect the legibility of the relay ramp, and (2) at depth, when a relay ramp is not entirely or is poorly imaged using a 2-D seismic cross-section, or 3-D seismic horizons.

7. Conclusion

In this paper three types of relay geometry are analysed: (i) open, (ii) linked and (iii) fully breached, in order to establish a linkage criterion. Statistics of parameters of relay ramps and comparison between displacement profiles of segmented faults and those of 'ideal isolated fault' are used to quantify and analyse the effect of displacement accumulation on fault linkage evolution. During fault interaction, displacement is redistributed along the whole fault segment array and especially at relay ramps. The profiles of the fault array are incoherent with the profile of an ideal isolated fault of the same length. After linkage, displacement is also redistributed along the entire fault array toward a displacement profile shape of an ideal isolated fault. This comparison of displacement profiles and the statistics of the parameters of the relay ramp show that *displacement* and *separation* are parameters significant of the linkage initiation and development between faults. Therefore, we represent the studied relay ramps on *relay displacement–separation* diagram, which reveals a specific field for each relay ramp type. The graphical field including all linked relays separates open and fully breached relays and is interpreted as a field of *relay displacement–separation* in which faults link during their overlap. This allows definition of a 'linkage threshold' for each studied fault system, which is the best-fit linear trend of linked relays. This analysis is completed with published data of relays of different scales and structural contexts. The whole dataset also defines a linear linkage threshold ($c^* = D/S$) varying less than one order in magnitude ($0.27 < c^* < 1$). This provides insight on scaling of relay ramps and suggests that linking relays have self-similar geometry between *relay displacement* and *separation* on a broad range of scale.

This work, which aims to improve the identification of relay ramp geometry, is important to resolve some problems related to the quality and the dimensions of the planes of inspection. For example, if a relay ramp is recognized but poorly imaged in a seismic reflection survey (Maerten et al., 2000), accurate characterization of its geometry could aid in identifying fluid leakage zones, and thus improve estimates of reservoir potential. Estimation of the relay ramp geometry can also be a good tool in evaluating a seismic hazard in a segmented seismic fault. Potential rupture surface should increase after fault segment linkage through a relay ramp (McLeod et al., 2000), which suggests that earthquakes could have larger magnitudes after linkage than before. The characterization of relay ramp geometry at the Earth's surface, where they are covered by sediment (e.g. Gawthorpe and Hurst, 1993; Gupta et al., 1999), or at depth using seismic survey data can also be a useful tool to estimate if a rupture can occur on only one segment (low earthquake magnitude) or on two or more segments (higher magnitude), as in the case of the Landers 1992 earthquake (Sieh et al., 1993).

Acknowledgements

The authors wish to thank Laurent Maerten for the constructive critical reading of an earlier version, and

Pierre Vergely for discussions and advice. Also thanks to Thierry Rives from Total for his encouragement to the realisation of this study. Thoughtful reviews by Alan Morris, David Peacock and David Ferrill helped to improve the quality of the manuscript. Field assistance and kindness of Francisco Gonzalez Lodeiro and Jesus Galindo-Zaldívar from the University of Granada were greatly appreciated during the course of the fieldwork.

References

Accocella, V., Gudmundsson, A., Funiciello, R., 2000. Interaction and linkage of extension fractures and normal faults: examples from rift zone of Iceland. Journal of Structural Geology 22, 1233–1246.

Ackermann, R.V., Schlische, R.W., Withjack, M.O., 2001. The geometric and statistical evolution of normal fault systems: an experimental study of the effects of mechanical layer thickness on scaling laws. Journal of Structural Geology 23, 1803–1819.

Alfaro, P., Galindo-Zaldivar, J., Jabaloy, A., Lopez-Garrido, A.C., Sanz de Galdeano, C., 2001. El sector de el Padul-Nigüelas, in: Sanz de Galdeano, C., Pelaez Montilla, J.A., Lopez Garrido, A.C. (Eds.), La Cuenca de Granada, Estructura, Tectonica Activa, Sismicidad, Geomorphologia y Dataciones Existents. CSIC, Universidad de Granada, pp. 121–132.

Aydin, A., Nur, A., 1982. Evolution of pull-apart basin and their scale independence. Tectonics 1, 91–105.

Aydin, A., Schultz, R.A., 1990. Effect of mechanical interaction on the development of strike-slip fault with en echelon patterns. Journal of Structural Geology 12, 123–129.

Bürgmann, R., Pollard, D.D., Martel, S.J., 1994. Slip distributions on faults: effects of stress gradients, inelastic deformation, heterogeneous host-rock stiffness, and fault interaction. Journal of Structural Geology 16, 1675–1690.

Cartwright, J.A., Mansfield, C., Trudgill, B., 1996. The growth of normal fault by segment linkage, in: Buchanan, P.G., Nieuwland, D.A. (Eds.), Modern Developments in Structural Interpretation, Validation and Modelling Geological Society Special Publication, 99, pp. 163–177.

Childs, C., Watterson, J., Walsh, J.J., 1995. Fault overlap zones within developing normal fault system. Journal of the Geological Society, London 152, 535–549.

Childs, C., Watterson, J., Walsh, J.J., 1996. A model for the structure and development of fault zones. Journal of the Geological Society of London 153, 337–340.

Cladouhos, T.T., Marret, R., 1996. Are fault growth and linkage models consistent with power-law distributions of fault lengths? Journal of Structural Geology 18, 281–293.

Collier, R.E.L., Pantosi, D., D'Addezio, G., De Martini, P.M., Masana, E., Sakellariou, D., 1998. Paleoseismicity of the 1981 Corinth earthquake fault, Seismic contribution to extensional strain in central Greece and implications for seismic hazard. Journal of Geophysical Research 103, 30001–30019.

Contreras, J., Anders, M.H., Scholz, C.H., 2000. Growth of normal fault system: observation of the Lake Malawi basin of the East African Rift. Journal of Structural Geology 22, 159–168.

Cowie, P.A., 1998. A healing–reloading feedback control on the growth rate of seismogenic faults. Journal of Structural Geology 20, 1075–1087.

Cowie, P., Roberts, G.P., 2001. Constraining slip rates and spacing for active normal faults. Journal of Structural Geology 23, 1901–1915.

Cowie, P.A., Shipton, Z., 1998. Fault tip displacement gradients and process zone dimensions. Journal of Structural Geology 20, 983–997.

Crider, J.G., Pollard, D.D., 1998. Fault linkage: three-dimensional mechanical interaction between echelon normal fault. Journal of Geophysical Research 103, 24373–24391.

Dawers, N.H., Anders, M.H., 1995. Displacement length scaling and fault linkage. Journal of Structural Geology 17, 607–614.

Dawers, N.H., Anders, M.H., Scholz, C.H., 1993. Growth of normal faults: displacement–length scaling. Journal of Structural Geology 21, 1107–1110.

Doblas, M., Oyarzun, R., 1989a. Neogene extensional collapse in the western Mediterranean (Betic–Rif Alpine Orogenic belt): implication for the genesis of the Gibraltar Arc and magmatic activity. Geology 17, 430–433.

Doblas, M., Oyarzun, R., 1989b. 'Mantle core complexes' and neogene extensional tectonics in the western Betic cordilleras, Spain: an alternative model for the emplacement of the Ronda peridotite. Earth and Planetary Science Letters 93, 76–84.

Doblas, M., Mahecha, V., Hoyos, M., Lopez-Ruiz, J., 1997. Slickenside and fault surface kinematic indicators on active normal faults of the Alpine Betic cordillera, Granada, Southern Spain. Journal of Structural Geology 19, 159–170.

Ferrill, D.A., Morris, A.P., 2001. Displacement gradient and deformation in normal fault system. Journal of Structural Geology 23, 619–638.

Ferrill, D.A., Stamatakos, J.A., Sims, D., 1999. Normal fault corrugation: implication for growth and seismicity of active normal faults. Journal of Structural Geology 21, 1999.

Gawthorpe, R.L., Hurst, J.M., 1993. Transfer zone in extensional basins: their structural style and influence on drainage development and stratigraphy. Journal of the Geological Society of London 150, 1137–1152.

Gupta, A., Scholz, C.H., 2000. A model of normal fault interaction based on observation and theory. Journal of Structural Geology 22, 865–879.

Gupta, S., Underhill, J.R., Sharp, I.R., Gowthorpe, R.L., 1999. Role of fault interaction in controlling synrift sediment dispersal patterns: Miocene, Abu Alaqa Group, Suez Rift, Sinai, Egypt. Basin Research 11, 167–189.

Huggins, P., Watterson, J., Walsh, J.J., Childs, C., 1995. Relay zone geometry and displacement transfer between normal faults recorded in coal-mine plans. Journal of Structural Geology 17, 1741–1755.

Jackson, J.A., Gagnepin, J., Houseman, G., King, G.C.P., Papadimitriou, P., Soufleris, C., Virieux, J., 1982. Seismicity, normal faulting, and the geomorphological development of the Gulf of Corinth (Greece: the Corinth earthquakes of February and March 1981). Earth and Planetary Science Letters 57, 377–397.

Kattenhorn, S.A., Aydin, A., Pollard, D.D., 2000. Joints at high angles to normal fault strike: an explanation using 3D numerical model of fault-perturbated stress field. Journal of Structural Geology 22, 1–23.

Larsen, P.H., 1988. Relay structures in a Lower Permian basement-involved extension system, East Greenland. Journal of Structural Geology 10, 3–8.

Maerten, L., Pollard, D.D., Karpuz, R., 2000. How to constrain 3-D fault continuity and linkage using reflection seismic data: a geomechanical approach. American Association of Petroleum Geologist Bulletin 84, 1311–1324.

Maerten, L., Gillepsie, P., Pollard, D.D., 2002. Effect of local stress perturbation on secondary fault development. Journal of Structural Geology 24, 145–153.

Manighetti, I., King, G.C.P., Gaudemer, Y., 2001. Slip accumulation and lateral propagation of active normal faults in Afar. Journal of Geophysical Research 106, 13667–13696.

Mansfield, C., Cartwright, J., 2001. Fault growth by linkage: observations and implications from analogue models. Journal of Structural Geology 23, 745–763.

Marchal, D., 1997. Approche spatio-temporelle des méchanismes de la propagation des failles normales: des modélisations analogiques à la sismique 3D. Ph.D. thesis, Université Henry Poincaré-Nancy I.

Marchal, D., Guiraud, M., Rives, T., 2003. Geometric and morphologic evolution of normal fault planes and traces from 2D to 4D data. Journal of Structural Geology 25, 135–158.

McLeod, A., Dawers, N.H., Underhill, J.R., 2000. The propagation and linkage of normal faults: insight from the Strathspey–Brent–Statfjord fault array, northern North Sea. Basin Research 12, 263–284.

Morley, C.K., 1999. Patterns of displacement along large normal faults: implication for basin evolution and fault propagation, based on examples from East Africa. The American Association of Petroleum Geologist Bulletin 83, 613–634.

Morley, C.K., Nelson, R.A., Patton, T.L., Munn, S.G., 1990. Transfer zones in the East African Rift System and their relevance to hydrocarbon exploration in rifts. The American Association of Petroleum Geologist Bulletin 74, 1234–1253.

Muraoka, H., Kamata, H., 1983. Displacement distribution along minor fault traces. Journal of Structural Geology 5, 483–495.

Nicol, A., Watterson, J., Walsh, J.J., Childs, C., 1996. The shapes, major axis orientations and displacement patterns of fault surfaces. Journal of Structural Geology 18, 235–248.

Palmer, A.C., Rice, J.R., 1972. The growth of slip surfaces in the progressive failure of over-consolidated clay. Proceeding of the Royal Society of London A332, 527–548.

Peacock, D.C.P., 2002. Propagation, interaction and linkage in normal fault system. Earth-Science Reviews 58, 121–142.

Peacock, D.C.P., Parfitt, E.A., 2002. Active relay ramp and normal fault propagation on Kilauea Volcano, Hawaii. Journal of Structural Geology 24, 729–742.

Peacock, D.C.P., Sanderson, D.J., 1991. Displacement, segment linkage and relay ramps in normal fault zones. Journal of Structural Geology 13, 721–733.

Peacock, D.C.P., Sanderson, D.J., 1994. Geometry and development of relay ramps in normal fault systems. The American Association of Petroleum Geologist Bulletin 78, 147–165.

Peacock, D.C.P., Sanderson, D.J., 1996. Effects of propagation rates on displacement variations along faults. Journal of Structural Geology 18, 311–320.

Pollard, D.D., Segall, P., 1987. Theoretical displacements and stresses near fractures in rocks: with applications to faults, joints, veins, dikes, and solution surfaces, in: Atkinson, B.K. (Ed.), Fracture Mechanics of Rock. Academic Press, London, pp. 277–349.

Roberts, G.P., Koukouvelas, I., 1996. Structural and seismological segmentation of the Gulf of Corinth fault system: implication for models of fault growth. Anali de Geofisica XXXIX 3, 619–646.

Scholz, C.H., Gupta, A., 2000. Fault interaction and seismic hazard. Journal of Geodynamics 29, 459–467.

Schultz, R.A., 2000. Fault–population statistics at the Valles Marineris Extensional Province, Mars: implication for segment linkage, crustal strain, and its geodynamical development. Tectonophysics 316, 169–193.

Schultz, R.A., Fossen, H., 2002. Displacement–length scaling in three dimensions: the importance of aspect ratio and application to deformation bands. Journal of Structural Geology 24, 1389–1411.

Segall, P., Pollard, D.D., 1980. Mechanics of discontinuous faults. Journal of Geophysical Research 85, 4337–4350.

Sieh, K., Jones, L., Hauksson, E., Hudnut, K., Eberthart-Philips, D., Heaton, T., Hough, S., Kanamori, H., Lilje, A., Lindvall, S., McGill, S.F., Mori, J., Rubin, C., Spotila, J.A., Stock, J., Kie Thio, H., Treiman, J., Wernicke, B., Zachariasen, J., 1993. Near-field investigations of the Landers Earthquake sequence, April to July 1992. Science 260, 171–176.

Trudgill, B., Cartwright, J., 1994. Relay ramp forms and normal-fault linkages, Canyonlands National Park, Utah. Geological Society of America Bulletin 106, 1143–1157.

Vergés, J., Martinez-Rius, A., 1988. Corte compensado del Pireneo oriental: geometria de las cuencas de ante-paisy edades de empezamiento de los mantos de corrimiento. Acta Geologia Hispanica 23, 95–106.

Walsh, J.J., Watterson, J., 1987. Distribution of cumulative displacement and seismic slip on a single normal fault surface. Journal of Structural Geology 9, 1039–1046.

Walsh, J.J., Bailey, W.R., Childs, C., Nicol, A., Bonson, C.G., 2003. Formation of segmented normal faults: a 3-D perspective. Journal of Structural Geology 26, 399–400.

Wesnousky, S.G., 1986. Earthquakes, quaternary faults, and seismic hazard in California. Journal of Geophysical Research 91, 12587–12631.

Willemse, E.J.M., 1997. Segmented normal faults: correspondence between three-dimensional mechanical models and field data. Journal of Geophysical Research 102, 675–692.

Willemse, E.J.M., Pollard, D.D., Aydin, A., 1996. Three-dimensional analyses of slip distributions on normal fault arrays with consequences for fault scaling. Journal of Structural Geology 18, 295–309.

Wojtal, S.F., 1996. Change in fault displacement population correlated to linkage between faults. Journal of Structural Geology 18, 265–279.

Young, M.J., Gawthorpe, R.L., Hardy, S., 2001. Growth and linkage of a segmented normal fault zone; the late Jurassic Murchinson–Statfjord North Fault, northern North Sea. Journal of Structural Geology 23, 1933–1952.